

# Optimal Progressive Image Transmission Over Rayleigh Fading Channels

Ahmad Hatam and Ali M. Doost-Hoseini

Department of Electrical and Computer Engineering, Isfahan University of Technology Isfahan, IRAN

## Summery

A fixed-packet optimal joint source channel coding scheme for transmission of progressive images over Rayleigh channels is proposed. A first order Markov model is used in rate allocation problem to concern channel temporal variations during image transmission. Also, introducing a modification on the used progressive coding scheme, the requirement for the immediate decoding termination upon the observation of an erroneous packet is relatively relaxed. A rate allocation mechanism for this modified version of progressive codes is also proposed.

## Key words:

Joint source channel coding , Markov model, Rayleigh fading channel, Rate allocation.

## 1. Introduction

Although independent optimizations of lossless source and channel coding operations in digital communication systems are globally optimal, it is shown that joint source/channel coding (JSCC) has better performance in the lossy image compression and transmission [1]. In JSCC, the compression ratio in the lossy source encoding and the channel code rates of the resulting packets are chosen such that some cost function is optimized under a constraint on either average transmission rate ( $TR$ ) in bits per pixel( $bpp$ ). This procedure is called rate allocation (RA). A well-known cost functions is mean distortion. Minimizing the mean distortion leads to distortion optimal (DRA) approach. If the transmitted packets have the same information component with various channel code words lengths, RA method is called variable-length packet coding (VLC). On the other hand, with a fixed channel code word length and variable information component, it is called fixed-length coding (FLC). Since fixed length packet is preferred in some applications such as the IP and ATM, our rate allocation approach is based on FLC configuration.

Progressive image coding that is used widely in JSCC, allows delay-free decoding of the received data and provides comfortable compression ratio adjustment. The quality of the reconstructed image improves as more data packets are received correctly. Nonetheless, if the decoding continues after an erroneous frame, the reconstructed image fidelity may deteriorate as more packets arrive. We assume that the channel decoder is

able to detect all errors and discard the first erroneous and all subsequent packets to prevent error propagation and a possible synchronization loss.

Some methods have been proposed to reduce the computational complexity of the DRA problem for the FLC. Banister *et al.* [2] presented a suboptimal DRA that is based on the Viterbi algorithm with  $O(N^2)$  complexity, where  $N$  is the number of the transmitted packets. Hamzaoui *et al.* [3] proposed a suboptimal method on the basis of a local search in the neighborhood of a rate optimal solution of [4]. In [5], with a special trellis, an optimal method is presented with complexity  $O(N^2)$ . Since the optimum trajectory on the trellis is found from the last packet back to the first one, it is called Back Trellis (BT) method. All the above works, indeed, are specialized to BSC channels. Pan *et al.* [7] proposed a suboptimal DRA in VLC under some restrictions for Rayleigh fading channels. They used a powerful rate-compatible LDPC code. They used average SNR, for computing packet decoding error probability (PDEP). One method for the consideration of the channel temporal variations is the Markov modeling [8-14]. Nosratinia *et al.* [15] have used a Gilbert-Elliott (2 state Markov model) for fading channels. They showed that if the encoder doesn't know the actual state transition instants, the worst-case base RA leads to a better mean distortion. Proposing a first order Markov model for the channel, Liu *et al.* [10] presented a suboptimal distortion optimal solution for FLC in fading channels. Each state of their model is realized by a BSC with crossover probability equal the average bit error rate in that state. They have actually used the upper bounds of packet decoding error probability (PDEP). Their RA method is similar to the local search in [3].

In this work, we propose an adjustable PDEP approximation in solving RA problem in Rayleigh fading channels. For this purpose, we assume the channel can be presented with Markov model, in which each state is represented by a BSC. We offer a suitable method for the states bit error rates assignment and the corresponding PDEPs. Also, with a modification on the progressive image encoding in SPIHT, we relax the requirement for the prompt decoding termination upon the observation of

the first erroneous packet. In Section 2, rate allocation problem is described. The first order model for Rayleigh fading channels to be used in our simulations is explained in Section 3. Then RA steps for Markov channels are described in Section 4. Modified SPIHT and the related RA are presented in Section 5. Sections 6 and 7 include simulation results and conclusions, respectively.

## 2. Problem Statement

In this section, we consider DRA in progressive image transmission over Rayleigh fading channels. The distortion function of the progressive image encoder and the set of possible channel code rates,  $\mathfrak{R} = \{r_1, r_2, \dots, r_M\}$ , are assumed to be known. All channel code words have a fixed length  $L$  and different information block lengths. From the budget constraint, the maximum number of transmitted packets is  $N = \lfloor TR \cdot S / L \rfloor$  for an image with total  $S$  pixels.

Consequently, the aim of a DRA algorithm is to find the optimal channel coding rates  $r_{k1}, \dots, r_{kN}$   $r_{ki} \in \mathfrak{R}$  for  $1 < i \leq N$ , in order to minimize the reconstructed image mean distortion under the budget constraint.

The mean distortion of the reconstructed image is given by:

$$E_N(D) = D_0 P_{r_{k1}} + \quad (1)$$

$$\sum_{i=1}^{N-1} D_i P_{r_{k_{i+1}}} \prod_{j=1}^i (1 - P_{r_{kj}}) + D_N \prod_{j=1}^N (1 - P_{r_{kj}})$$

where  $D_i$  is the MSE distortion due to the first  $i$  packets and  $P_{r_{ki}}$  is the  $i$ th packet PDEP with channel coding rate  $r_{ki}$  ( $r_{ki} \in \mathfrak{R}$ ) and  $D_0$  is the corresponding MSE distortion when any packets aren't received correctly. For a constant channel,  $P_{r_{ki}}$  depends on the channel code rate  $r_{ki}$ , but for a time varying channel, it also depends on the packet number  $i$ .

In RA for varying channels, the approximate values of PDEP for all packets are needed. The finite state Markov model assumption helps in this regard. In our simulations, we use the first order Markov model for Rayleigh fading channel [8] with a minor modification in the states BER assignment. These are described in the following sections.

## 3. Finite State Markov Model

A finite state Markov model for a Rayleigh channel (FSMC) is described in this section [8-12]. In these channels, the received signal envelope,  $r$ , has Rayleigh

distribution and corresponding signal to noise ratio (SNR),  $\gamma$ , is exponentially distributed[16]:

$$p(\gamma) = \frac{1}{\gamma_0} e^{-\frac{\gamma}{\gamma_0}} \quad \gamma \geq 0 \quad (2)$$

where  $\gamma_0$  is the average SNR.

The SNR band is partitioned into  $K$  intervals, by the states thresholds vector  $\vec{\Gamma} = [\Gamma_1 = 0, \Gamma_2, \Gamma_3, \dots, \Gamma_K, \Gamma_{K+1}]$ .

The interval  $[\Gamma_k, \Gamma_{k+1})$  corresponds to  $k$ th state of the Markov model. The steady-state probability of the  $k$ th state,  $\pi_k$ , is given by:

$$\pi_k = \int_{\Gamma_k}^{\Gamma_{k+1}} p(\gamma) d\gamma = e^{-\frac{\Gamma_k}{\gamma_0}} - e^{-\frac{\Gamma_{k+1}}{\gamma_0}} \quad (3)$$

State thresholds may be derived from the following equations on the basis of equal average states occupancy duration,  $\bar{\tau}_k$ , assumption [8]:

$$\bar{\tau}_k = \frac{1}{\sqrt{2\pi} f_m} \frac{e^{-\frac{\Gamma_k}{\gamma_0}} - e^{-\frac{\Gamma_{k+1}}{\gamma_0}}}{\sqrt{\frac{\Gamma_{k+1}}{\gamma_0}} e^{-\frac{\Gamma_k}{\gamma_0}} + \sqrt{\frac{\Gamma_k}{\gamma_0}} e^{-\frac{\Gamma_{k+1}}{\gamma_0}}} \quad (4)$$

$$= C_P T_P$$

in which  $f_m$  is the maximum Doppler frequency shift.

Suitable values for  $C_P$  are between 3 and 8 [8]. For example, if  $f_m$  and  $T_P$  equal 4.16 Hz and 8.276 ms, respectively, and  $C_P$  is set equal to 3, the model ends up in 11 states. Table 1 shows the normalized upper SNR thresholds for this model.

Table 1: Normalized upper SNR thresholds for Markov states with  $C_P = 3$  and  $f_m T_P = 0.0344$

State $k$	1	2	3	4	5
$\gamma_u / \gamma_0$	0.01	0.11	0.34	0.70	1.19
State $k$	6	7	8	9	10
$\gamma_u / \gamma_0$	1.82	2.50	3.53	4.64	5.95

In FSMC, it is assumed that the transition occurs only between adjacent states. Hence,  $P_{trans}(i, j)$  is zero for  $|i - j| > 1$  and [12]:

$$P_{trans}(k, k+1) \approx \frac{\sqrt{\frac{2\Gamma_{k+1}}{\gamma_0}} f_m e^{-\frac{\Gamma_{k+1}}{\gamma_0}}}{\frac{\Gamma_k}{\gamma_0} e^{-\frac{\Gamma_k}{\gamma_0}} - \frac{\Gamma_{k+1}}{\gamma_0} e^{-\frac{\Gamma_{k+1}}{\gamma_0}}}, k=1, \dots, K-1 \quad (5)$$

$$P_{trans}(k, k-1) \approx \frac{\sqrt{\frac{2\pi}{\gamma_0}} f_m e^{\frac{\Gamma_k}{\gamma_0}}}{R_i(e^{\frac{\Gamma_k}{\gamma_0}} - e^{\frac{\Gamma_{k+1}}{\gamma_0}})}, \quad k=2, \dots, K \quad (6)$$

where  $R_i$  is the packet transmission rate and is the reciprocal of  $T_p$ .

Finally, using (6) and (7), the probability of remaining in the  $k$ th state becomes:

$$P_{trans}(k, k) = \begin{cases} 1 - P_{1,2} & k=1 \\ 1 - P_{k,k+1} - P_{k,k-1} & 1 < k < K \\ 1 - P_{K,K-1} & k=K \end{cases} \quad (7)$$

#### 4. RA Procedure

A finite state Markov model facilitates PDEP approximation required in RA. Assume that the channel model has  $K$  states with transition probability matrix  $P_{trans}$  and steady state probability vector  $\pi$ . We, further, assume the channel remains unchanged during a packet transmission. Also,  $\bar{P}_0$ , the initial state probability vector of the channel just before the beginning of the transmission is assumed to be known, or we set  $\bar{P}_0 = \pi$ .

On the basis of the above modeling and assumptions, RA consists of these steps:

- 1) Each state is approximated by a fixed BSC with appropriate bit error rate ( $\varepsilon_k$  for  $k$ th state).
- 2) State probability vector during the  $i$ th packet transmission is approximated.
- 3) Approximate values of PDEPs are derived.
- 4) RA is performed by minimizing (1).

##### 4.1 States BER Assignment

Each state of the Markov model is approximated by a BSC model. Bit error rate (BER) of the  $k$ th state BSC,  $\varepsilon_k$ , depends on the state SNR interval and the modulating scheme. In [10],  $\varepsilon_k$  is approximated by the mean BER of the  $k$ th state:

$$\varepsilon_k = \frac{1}{\pi_k} \int_{\Gamma_k}^{\Gamma_{k+1}} p(\gamma) P_e(\gamma) d\gamma \quad (8)$$

Where  $P_e(\gamma)$  is the error probability as a function of the received SNR. For example, in BPSK,  $P_e(\gamma) = \text{erfc}(\gamma)$ .

The difference between the actual and approximate values of  $\varepsilon_k$  affects the performance efficiency of rate allocation. In [7] it is shown, through simulations, that

the performance loss is more noticeable, when the actual channel condition is worse than the approximated one. On this basis, we use the worst case SNR for the states bit error assignment in the present work:

$$\varepsilon_k = P_e(\Gamma_k) \quad (9)$$

Our observations verify that the worst case approximation is preferable over the averaging method. However, it is worth looking for better assignment procedures. Fig. 1 shows the worst case BER of the 11-state FMSC in Section 3 from (9) for some states. For each value of  $\gamma_0$ , the Markov states can be divided into “bad” (with high BER), “good” (with near zero BER) and “fair” groups. If we reduce the model states to these 3 categories, the resultant model is simpler, but less fine than the 11-states counterpart.

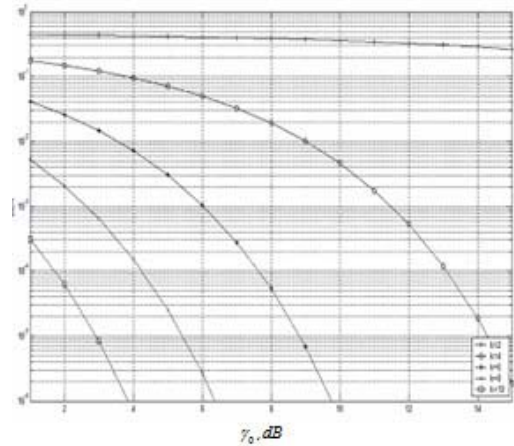


Fig. 1 Worst case BER of the equivalent BSCs of the Markov states.

##### 4.2 State Probability Vector

Assume that the channel state remains unchanged during the transmission of each packet. If state transition obeys a Markov model with transition probability matrix  $P_{trans}$ , then the state probability vector during the  $i$ th packet transmission,

$\bar{P}_i = (\bar{P}_i(1), \bar{P}_i(2), \dots, \bar{P}_i(K))$ , in which

$\bar{P}_i(k)$  is the probability of channel is in the  $k$ th state for the transmission period of packet number  $i$ , is:

$$\bar{P}_i = \bar{P}_{i-1} P_{trans} \quad i=1, \dots, N \quad (10)$$

##### 4.3 PDEP Approximation

Let  $P_{r_i}(\varepsilon_k)$  denote the probability of erroneous decoding of  $i$ th transmitted packet with channel code rate  $r_i$  ( $r_i \in \mathfrak{R}$ ) when the channel is in its  $k$ th state number and

bit error rate  $\varepsilon_k$ . Actual value of  $P_{r_i}$  may be one of  $P_{r_i}(\varepsilon_1), P_{r_i}(\varepsilon_2), \dots, P_{r_i}(\varepsilon_K)$  with probabilities of  $\bar{P}_i(1), \bar{P}_i(2), \dots, \bar{P}_i(K)$ , respectively. We propose the following average PDEP (AVP) as an approximation of  $P_{r_i}$ :

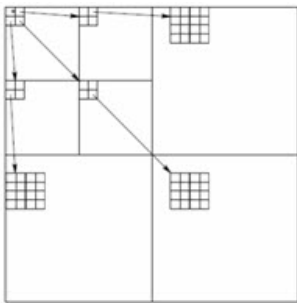
$$P_{r_i} = \sum_{k=1}^K P_{r_i}(\varepsilon_k) \bar{P}_i(k) \quad (11)$$

At this point, we can minimize (1) by optimal BT algorithm [5] or fast suboptimal local search algorithm [3], depending on the application.

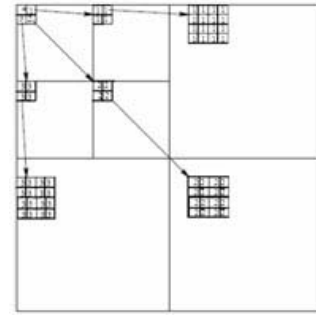
The above discussion can be applied in any finite state Markov channel with fixed average states occupancy duration. However, our simulations are on the basis of finite states Markov model in Section 3.

## 5. Layered SPIHT (LSPIHT)

SPIHT is a wavelet transform based image coding algorithm [17]. The underlying idea for the compression in SPIHT is the application of a significance function on each set of pixels. It is one if the maximum value of the pixels in a set is greater than some threshold, and zero otherwise. The insignificant sets are encoded by fewer bits. In this algorithm, the image wavelet transform coefficients are partitioned using a hierarchical tree as in Fig. 2(a). The tree roots are the pixels in the highest level that are grouped in  $2 \times 2$  adjacent pixels. Each pixel in a group, except one in the top left corner, has four descendants. Each of the pixels in other levels, except those in lowest one, has also four descendants. The compression procedure of SPIHT consists of two stages of sorting pass and refinement pass with the first being the main one. These passes are repeated from the most significant bit-plane of the coefficients toward the least significant one. Three lists are used in the encoding algorithm: List of insignificant pixels (LIP), List of insignificant sets (LIS) and List of significant pixels (LSP). LIS entries refer to their descendants and are indicated by type A or B, if they refer to all or merely indirect descendants, respectively.



(a) Typical structure of a SPIHT tree



(b) Typical structure of LSPIHT trees labeled by 1, 2 and 3

Fig. 2 Comparison of typical trees structures SPIHT and LSPIHT

The sorting pass for each bit-plane checks LIP and LIS. Briefly, in this stage insignificant and significant entries of these Lists are searched. Insignificant sets are encoded by a few bits and significant ones are moved to LSP to be encoded in the refinement pass. If the decoder duplicates the execution passes of the encoder, it can reconstruct the image. The quality of the reconstructed image increases as more bits are decoded, but the decoding must stop if an erroneous packet is detected. In LSPIHT, we have tried to relax this restriction. LSPIHT can be viewed as a layered version of the SPIHT. Many of their features are similar and we emphasize on the differences. First, the tree in the original SPIHT is partitioned into three sub-trees. The root of each tree, as shown in Fig. 2(b), corresponds to one of the  $2 \times 2$  adjacent pixels in Fig. 2(a), except the one with star. The starred pixel maybe referred to each of the trees. The algorithm compresses along each sub-tree with its own lists by SPIHT algorithm. So LSPIHT encodes image in three separate bitstreams or layers that can be decoded independently from each other. If the decoding stops due to an error in one layer, it continues in other layers. Clearly, each bitstream needs a label to identify its layer number for the decoder. The order number and the length of a layer, embedded in the header of the final bitstream, must be protected highly enough to ensure correct reception. The packets corresponding to these three layers may be interleaved, in the order of their effects in mean distortion reduction, to ensure the progressive nature of the final bitstream.

### 5.1 Rate allocation in LSPIHT

RA in LSPIHT is carried out in roughly three steps: Layer budget assignment, Layer rate allocation, Interleaving. In the first step, the simplest form of the budget assignment to layers is equal proportions. A better

approach is based on the data volume in each layer. None of these methods incorporates the importance of a layer. A budget allocation procedure is proposed with this consideration. It is comprised of these stages: In the first stage, all layers are partitioned into equal small size units. Then, the units in all layers are arranged in a queue, of length  $B$ , in the descending order of MSE distortion reduction. Finally, the number of the units from each layer in the queue determines its budget. Clearly, the units' length affects the assignment quality. A smaller size leads to a more accurate assignment, but increases the processing time. Although, this queue provides the pseudo-progressive code, but introduces greater redundancy needed to distinguish the units layers in the packets. After the budget assignment, in the second step rate allocation in each layer is performed separately.

For keeping the progressive property on the packet level, all packets are interleaved in the third step on the basis of their importance in MSE distortion reduction.

## 6. Simulations

In our simulations, a progressively coded bitstream is transmitted over a Rayleigh fading channel after the rate allocation. Images are compressed according to the coding procedures existing in SPIHT or the proposed LSPIHT. We use rate compatible punctured turbo codes (RCPT) of [18], [2]. All channel codewords are 4138 bits long, with 7 possible rates 4/12, 5/12, 6/12, 7/12, 8/12, 9/12, 10/12, 11/12. Each packet with rate  $r$  contains 16 bits for the CRC and an 8 bit header to specify  $r$ . Hence, the information content of a packet is  $(4138r - 24)$  bits.

We use  $512 \times 512$  8 *bpp* images in our simulations. For a target transmission rate of 0.252 *bpp*, the number of the transmitted packets for each image will be 16.

The entire image transmission-reception system through a Rayleigh fading channel with the following specification is simulated by Matlab. The simulation parameters are as follows: Modulation scheme: BPSK, Carrier frequency: 900 MHz,

Max speed: 5km/h ( $f_m = 4.16\text{Hz}$ ), Transmission rate: 500Kb/s ( $T_p = 8.276\text{ ms}$ ).

With these values of  $f_m$  and  $T_p$ , the resulting FSMC consists of 11 states. Assuming  $\gamma_0$  and the initial channel state (ICS) are known at the transmitter, following a PDEP approximation, the Back-Trellis algorithm of [5] is used for RA in each image. The image SPIHT bit stream is packetized and channel coded according to the allocated RCTP rates, modulated and sent over the Rayleigh channel. The iterative decoding of the received packets are performed 20 times. The packets CRCs are checked to detect possible decoding error. Decoding is stopped

wherever an erroneous packet is detected. Finally, the image is reconstructed from the resultant decoded stream with inverse SPIHT coding scheme. The peak signal to noise ratio (PSNR) criterion is used to assess the quality of the reconstructed image. The PSNR of a reconstructed 8 bits per pixel image with MSE distortion  $D$  is defined by [17]:

$$PSNR = 10 \log_{10} \left( \frac{255^2}{D} \right) \quad (12)$$

The performance evaluations are performed separately on "Lena", "Barbara" and "Goldhill" images by averaging the PSNR of the reconstructed images from 1000 repetitions of each simulation. Since the results are quite consistent, we present those of "Lena" only.

### A. AVP Performance Comparison

We compare the proposed PDEP approximation method with two other works ([7],[10]) under similar conditions. In [7], the average SNR have used for RA but haven't addressed SNR fluctuations in different packets for PDEP approximation in the solution of DRA problem. On the other hand, in [10] they have used the upper bounds of PDEP approximation. Fig. 3 shows the results for two known ICS. The PSNR performance is improved when  $\gamma_0$  increases or ICS is better, as shown in Fig.3 (b). It also shows that the RA based on AVP outperforms the two other methods. The PSNR difference is more obvious for lower values of  $\gamma_0$ . In these states, the equivalent BERs, as well as PDEPs, are high and the probability of packet failure is high, too. On the other hand, Fig. 3 shows that for high values of  $\gamma_0$ , the qualities of the reconstructed image are similar. This happens because in these cases, almost all packets are decoded correctly.

### B. States BER Assignment

In this step, we compare the worst case and averaged bit error rate schemes. The PSNR difference in these methods is less than 0.04 dB for the 11- state Markov model. This is a well-expected result since for narrow SNR bands, the approximations are almost the same. For further clarity, we use a Markov channel with wider SNR bands (with corresponding wider BER ranges). This is done by merging each three adjacent states of the 11-state Markov model. Fig. 4 shows the PSNR performance results for this new 4-state Markov model. The ICS is two in Fig. 4(a) and four in Fig. 4(b). Merged ICS of two has a wider SNR band than ICS of four. The PSNR difference in Fig. 4(a) with ICS of two is more visible. In the Fig. 4(a) ICS of four is a good initializing state in which the BER values are low and the band is narrow leading to a negligible approximation

difference between two assignments. From this comparison, we conclude that the proposed approach

manifests a better performance, especially for wide SNR bands.

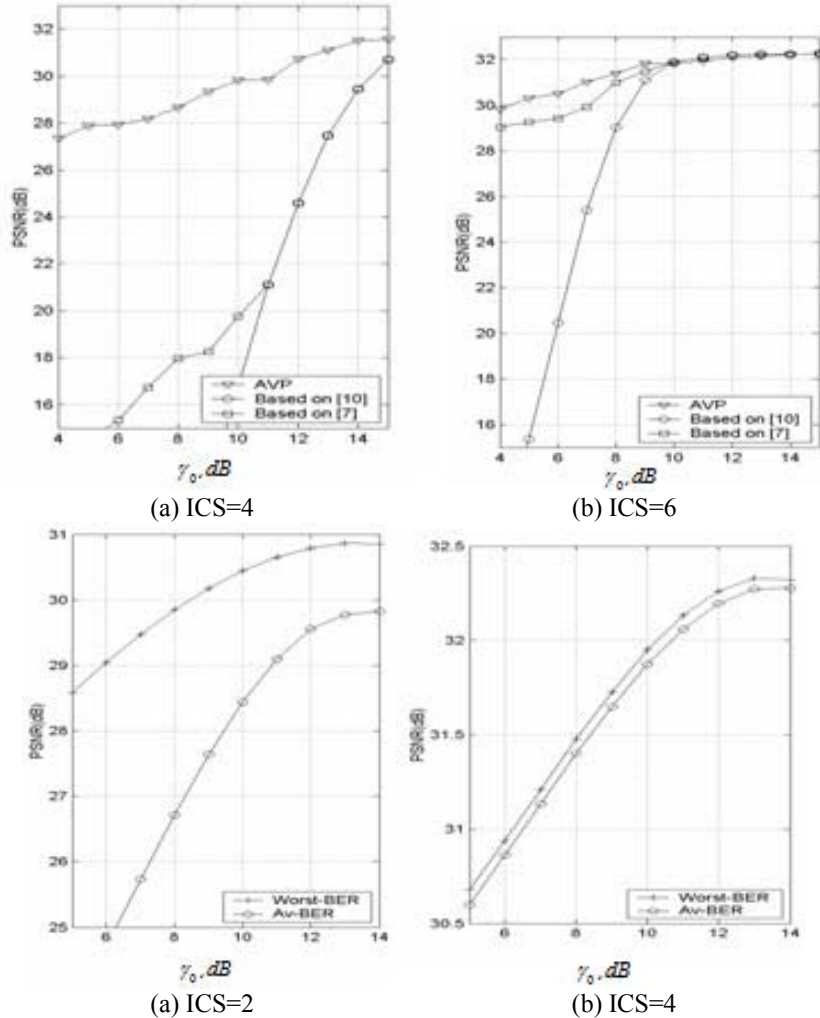


Fig. 4 PSNR comparison of "Lena" image for two BER approximations in the 4-state Markov model

### C. Markov states reduction

In order to observe the effect of states merging, we compare the PSNR performances for two ICSs in 11-states Markov model with the same ICS in its merged 4-states feature. Fig. 5 shows the results. The designated ICS values refer to the 11- and 4- states models, respectively. The ICS in the latter model is two which value corresponds to ICS values from four to six in the original 11-state version. The resultant rates only differ for the 11-state model, in Figs. 5(a) and 5(b). It is observed that merging states leads to PSNR loss which is greater in Fig. 5(b), because of a better ICS in the fine model. Hence, although the reduction of the number of

states reduces the computations, the consequent PSNR loss is not negligible.

### D. Application of LSPIHT

In this step, we compare the performances of our proposed LSPIHT and original SPIHT algorithms. LSPIHT requires an extra 10 bits overhead in which the two layer identifier bits are highly protected by five repetitions. Therefore, the actual information content of a packet is  $(4138r - 34)$  bits in this case. Fig. 6 shows the simulation results. We observe that when  $\gamma_0$  is low and channel is in a bad condition (Fig. 2), LSPIHT achieves a large PSNR gain over SPIHT. This is because

in such cases, the packet error rates are high and the decoding ceases relatively soon with the first erroneous packet in SPIHT. On the contrary, in LSPHIT the decoding continues until an error occurs in all layers. As  $\gamma_0$  increases, the channel moves towards good states and the PSNR difference between LSPHIT and SPIHT vanishes. If  $\gamma_0$  passes the threshold of Fig. 6, LSPHIT

loses its advantage. Note that the PSNR losses in these cases are less than 0.5 dB. If a 0.5 dB PSNR loss is not important for an application, or if the channel is usually in bad states, LSPHIT is desirable. Intelligent switching between LSPHIT and SPIHT, on the basis of the channel condition, seems to be a valuable compromise.

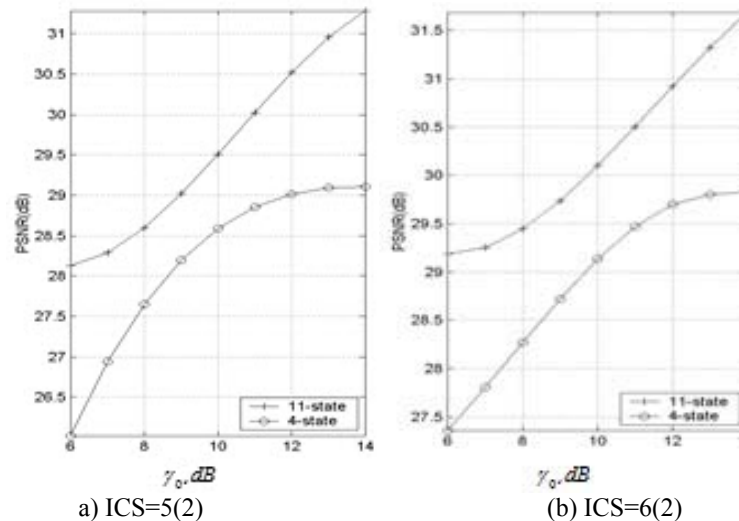


Fig. 5 PSNR comparison of "Lena" image for 11- and 4-states Markov models.

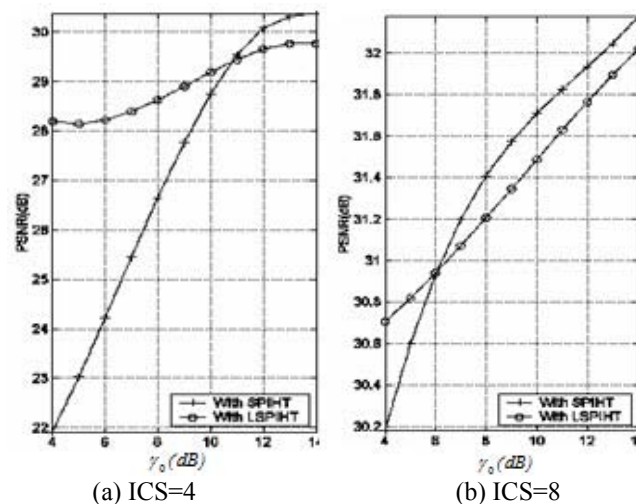


Fig. 6 PSNR comparison of "Lena" image between SPIHT and LSPHIT.

## 7. Conclusions

We presented a method for rate allocation problem in progressive image transmission over Markov channels. We used the finite state Markov modeling of [8] for the time varying Rayleigh fading channels in our

simulations, but we used the worst case BER for each states to obtain performance improvement over the existing averaging scheme. Also, through simulations, we showed that the proposed AVP method for PDEP approximations, works well in rate allocation. Also we offered a modified layered version of SPIHT and



proposed a rate allocation procedure in this case. We observed that LSPIHT leads to a noticeably better performance in a noisy channel. Although a Rayleigh fading channel with first order Markov model is used in our discussions, the proposed rate allocation method can be extended to other varying channel with higher order Markov models.

## References

- [1] Sherwood P. G., Zeger K., "Progressive image coding for noisy channels," IEEE Signal Processing Letters, vol. 4, no. 7, pp. 189-191, 1997.
- [2] Banister B. A., Belzer B., and Fischer T. R., "Robust image transmission using JPEG2000 and turbo-codes," IEEE Signal Processing Letters, vol. 9, no. 4, pp. 117-119, 2002.
- [3] Hamzaoui R., Stankovic V., and Xiong Z., "Rate-based versus distortion-based optimal joint source-channel coding," Proc. IEEE DCC, pp. 63-67, 2002.
- [4] Stankovic V., Hamzaoui R., Saupe D., "Fast Algorithm for Rate-Based Optimal Error Protection of Embedded Codes," IEEE Trans. On Comm., vol. 51, no. 11, pp. 1788-1795, 2003.
- [5] Banihashemi A.H., Hatam A., "A Distortion optimal rate allocation algorithm for transmission of progressive bitstreams over noisy channels," IEEE Trans. On Comm., vol. 56, no. 10, pp. 1581-1584, 2008.
- [6] Chande V., and Farvardin N., "Progressive transmission of images over memoryless noisy channels," IEEE Journal And Selected Areas In Comm. , vol. 18, no. 6, pp. 850-860, 2000.
- [7] Pan X., Banihashemi A. H., Cuhadar A., "Progressive transmission of images over fading channels using rate-compatible LDPC codes," IEEE Trans. On image proc., vol. 15, no. 12, pp. 3627-3635, 2006.
- [8] Zhang Q., Kassam S.A., "Finite-state Markov model for Rayleigh fading channels," IEEE Trans. On Comm., vol. 47, no. 11, pp. 1688-692, 1999.
- [9] Turin W, Nobelen R.V., "Hidden Markov modeling of flat fading channels," IEEE Journal And Selected Areas In Comm., vol. 16, no. 9, pp. 1809-1817, 1998.
- [10] Liu Z., Zhao M., Xiong Z., "Efficient Rate Allocation for Progressive Image Transmission via Unequal Error Protection Over Finite-State Markov Channels," IEEE Trans. On Signal Proc., vol. 53, no. 11, pp. 4330-4338, 2005.
- [11] Annavajjala R., Chockalingam A., Cosman P. C., Milstein L.B., "First-order Markov models for packet transmission on Rayleigh fading channels with DPSK/NCISK modulation," IEEE Int. Symposium on Inf. Theory , Seattle, Washington, U.S.A. , pp. 2864-2868, 2006.
- [12] Wang H. Sh., Moayeri N., "Finite-state Markov channel- a useful model for radio communication channel," IEEE Trans. On Vehicular Tech., vol. 44, no. 1, pp. 163-171, 1995.
- [13] Kumwilaisak W., Kue J., Wu, D., "Fading channel modeling via variable-length Markov chain technique," IEEE Trans. On Vehicular Tech, vol. 57, no. 3, pp. 1338-1358, 2008.
- [14] Chung W. H., Yao K., "Modified hidden Semi-Markov model for modeling the flat fading channel," IEEE Trans. On Comm., vol. 57, no. 6, pp. 1806-1814, 2009.
- [15] Nosratinia A., Liu J., and Aazhang B., "Source-channel rate allocation for progressive transmission of images," IEEE Trans. On Comm., vol. 51, no. 2, pp. 186-196, 2003.
- [16] Goldsmith A., Wireless communications, Cambridge university press, First edn. , 2005.
- [17] Said A. and Pearlman W. A., "A new , fast and efficient image codec based on set partitioning in hierarchical trees," IEEE Trans. Circuits And Systems For Video Technology, 1996, vol. 6, no. 3, pp. 243-250, 1996.
- [18] Acikel O. F., Ryan W.E., "Punctured turbo-codes for BPSK/QPSK channels," IEEE Trans. On Comm., vol. 47, no. 9, pp. 1315-1323, 1999.